Journal of Infection 90 (2025) 106400

Contents lists available at ScienceDirect

Journal of Infection

journal homepage: www.elsevier.com/locate/jinf

Infectious Disease Practice

MicroRNA biomarkers and host response pathways in severe pulmonary hemorrhagic syndrome due to leptospirosis: A multi-omics study

Phu Nguyen Trong Tran [a,b,c], Umaporn Limothai [b,d], Janejira Dinhuzen [b,d], Sasipha Tachaboon [b,d], Theerapon Sukmark [e], Chayomon Dokpong [f], Sittiruk Roytrakul [g], David A. Haake [h,i], Nattachai Srisawat [a,b,d,j,k,l,*]

[a] Faculty of Medicine, Chulalongkorn University, Bangkok, Thailand
[b] Excellence Center for Critical Care Nephrology, King Chulalongkorn Memorial Hospital, Bangkok, Thailand
[c] Department of Internal Medicine, Faculty of Medicine, Can Tho University of Medicine and Pharmacy, Can Tho, Vietnam
[d] Tropical Medicine Cluster, Chulalongkorn University, Bangkok, Thailand
[e] Thungsong hospital, Nakhon Si Thammarat, Thailand
[f] Khukhan hospital, Sisaket, Thailand
[g] National Center for Genetic Engineering and Biotechnology (BIOTEC), Pathum Thani, Thailand
[h] Veterans Affairs Greater Los Angeles Healthcare System, Los Angeles, CA, USA
[i] The David Geffen School of Medicine, University of California, Los Angeles, CA, USA
[j] Division of Nephrology, Department of Medicine, Faculty of Medicine, King Chulalongkorn Memorial Hospital, Bangkok, Thailand
[k] Center for Critical Care Nephrology, The CRISMA Center, Department of Critical Care Medicine, University of Pittsburgh, School of Medicine, Pittsburgh, PA, USA
[l] Academy of Science, Royal Society of Thailand, Bangkok, Thailand

ARTICLE INFO

Article history:
Accepted 23 December 2024
Available online 8 January 2025

Keywords:
Leptospirosis
SPHS
Pulmonary hemorrhage
MicroRNA
Multi-omics
Biomarkers
Pathway analysis

SUMMARY

Background: Severe pulmonary hemorrhagic syndrome (SPHS) remains a fatal complication of leptospirosis with poorly understood mechanisms and an urgent need for effective biomarkers.
Methods: A nested case-control analysis was conducted using blood specimens from two previous Thai leptospirosis cohorts. Candidate microRNAs were initially discovered through a global profiling of 798 serum microRNAs in five SPHS and seven non-SPHS patients, and then validated using real-time polymerase chain reactions in 168 patients. Pathways enriched from microRNA targets were compared to those from an integrated transcriptomic-proteomic analysis. Proteins pertaining to the key resulting pathway were measured to validate significance and reveal correlation with microRNA biomarkers.
Results: Serum microRNA profiling revealed a total of 81 significantly expressed microRNAs, of which seven were selected for further validation in the whole cohort of 168 leptospirosis patients, including 28 in SPHS and 140 nonSPHS groups. Among the selected microRNAs, miR-5010–3p and miR-147b-3p had significantly higher expression in SPHS group compared to nonSPHS group, with consistently higher expression after adjusting for age, sex, days of illness, comorbidity, smoking status or recruitment site. The two had area under the curve (AUC) values of 0.76 (95% CI: 0.67–0.85) and 0.70 (95% CI: 0.56–0.81) for discriminating SPHS, respectively. These microRNAs also exhibited consistent AUC values in patients tested before chest radiograph shadows manifested. Combination of miR-5010–3p with miR-548ai and miR-224–5p, as selected by Bayesian Model Averaging algorithm, substantially boosts the AUC value to 0.86 (95% CI: 0.77–0.94). The miRNA biomarkers also enhanced the predictive values of a previously validated clinical model, increasing AUC value from 0.87 to 0.92 with a significant reclassification net index. Multi-omics pathway analysis incorporating microRNA targets and transcriptomic-proteomic data suggested TNF signaling as among the key pathways. In validation, seven out of ten pathway proteins were significantly different between groups, with principal components correlated with severity and miR-5010–3p.
Conclusions: MiR-5010-3p and miR-147b-3p are novel biomarkers with good predictability and potential relevance with TNF signaling pathway, an important host response mechanism in leptospirosis SPHS.

* Correspondence to: Excellence Center for Critical Care Nephrology, King Chulalongkorn Memorial Hospital, Khwaeng Pathum Wan, Pathum Wan, Bangkok 10330, Thailand.
E-mail address: nattachai.sr@chula.ac.th (N. Srisawat).

https://doi.org/10.1016/j.jinf.2024.106400

Introduction

Leptospirosis, a zoonotic disease endemic to many tropical regions, is among the most widespread zoonoses worldwide. It affects over one million patients annually and contributes to approximately 58,900 deaths and 2.90 million disability-adjusted life years worldwide.[1,2] Patients infected with *Leptospira* spp. may present with a wide spectrum of clinical symptoms, ranging from subclinical infection to mild disease to severe complications. Among these, severe pulmonary hemorrhagic syndrome (SPHS), characterized by alveolar hemorrhage, acute respiratory distress syndrome, and multi-organ failure, has been reported as the complication with the highest risk of death associated with leptospirosis.[3–5] Despite intensive treatment, the mortality rate linked to this syndrome can be as high as 50%.[6]

Early identification of SPHS is crucial for timely intervention and improved patient outcomes. However, the diverse clinical features of leptospirosis make it challenging to diagnose and predict disease severity at the onset of illness based on clinical assessment alone. Pulmonary hemorrhage could be present even in patients without any respiratory symptoms.[7] Chest radiography findings were found to be insensitive to alveolar hemorrhage and could not discriminate patients with SPHS at hospital admission.[8,9] Existing clinical models to detect pulmonary complications required many covariates, hindering their translation to clinical practice.[9,10]

The search for potential biomarkers that can serve as early warnings for disease severity and SPHS has been the topic of active research. A canine model study found association between the elevation of endothelial activation markers with SPHS.[11] In human, platelet-activating factor acetylhydrolase was elevated in patients infected by *L. interrogans* serovar Icterohaemorrhagiae and was suggested as marker of the syndrome.[12] Several cytokines, such as IL-5, IL-6, IL-8, IL-10, and MIF, were found to be significantly elevated in leptospirosis patients with SPHS.[13,14] Nevertheless, there remains an urgent need for validated biomarkers for human leptospiral SPHS.

MicroRNAs (miRNAs), a type of small non-coding RNA molecules, play essential roles in regulating various biological processes. Extracellular and circulating miRNAs, detectable in various types of body fluid, are of great interest as potential biomarkers for various diseases.[15] Besides their high accessibility and stability, these molecules are superior to whole blood miRNAs since their expression pattern is less prone to blood cell interference.[16] In tropical infectious diseases such as dengue and leptospirosis, previous studies have demonstrated the ability of miRNAs to predict severe outcomes.[17,18] Leveraging the biorepository from two large and well-characterized multi-center cohorts of leptospirosis patients in Thailand, we conducted this study to explore the potential of miRNAs as novel biomarkers for SPHS and unravel their biological relevance through a multi-omics approach.

Methods

Study design and participants

This was a nested case-control analysis of a previous multi-center cohort study conducted in 15 hospitals in Sisaket province, northern Thailand from December 2015 to November 2018 and an ongoing cohort starting from 2019 in 8 hospitals in Sisaket and Nakhon Si Thammarat province (southern Thailand). All participants had given their consent regarding the use of remnant samples for further studies. The current study has received Institutional Review Board approval (IRB No.0576/66), Faculty of Medicine, Chulalongkorn University. A detailed description of the first cohort has been published elsewhere.[19]

All the included patients had signs and symptoms suggestive of leptospirosis, including acute febrile illness, headache, and myalgia with history of exposure to animal water reservoirs or flooded environments either at home or at work, and had confirmed leptospirosis by one or more of the following methods: (1) microscopic agglutination test (MAT) with positive results defined as a single titer at least 400 or a four-fold increase between acute and convalescent phases, (2) positive quantitative polymerase chain reaction (qPCR) assay for pathogenic *Leptospira* spp. in blood, or (3) positive blood culture.

All patients' specimens were collected immediately after written consents were obtained, usually within 24 h of admission. At each site, the specimens were processed according to a common protocol and shipped to the Center for Excellence in Critical Care Nephrology, King Chulalongkorn Memorial Hospital for storage at −80^{0}C until analysis (S-Fig. 1, Supplementary materials).

Leptospirosis severe pulmonary hemorrhagic syndrome (SPHS) was defined as the presence of severe acute respiratory failure with diffuse alveolar infiltrates on chest radiograph, or with hemoptysis or fresh blood in endotracheal suction, in a patient with a confirmed diagnosis of acute leptospirosis.[20,21] Controls (non-SPHS) were patients who did not develop any signs of SPHS throughout the hospitalization course. The research team prospectively followed and evaluated the patients every day to detect SPHS and assess outcomes. All patients were managed in accordance with the current guidelines for leptospirosis from the Department of Disease Control, Ministry of Public Health of Thailand.

Sample size was calculated for the main objective, which was to validate miRNA biomarkers discriminatory performance. A total of 168 patients, including 28 SPHS and 140 randomly-selected non-SPHS patients, were analyzed. Justification for the sample size in Nanostring nCounter® and RT-qPCR experiment was detailed in the Supplementary materials (Section 2, S-Table 1 and S-Fig. 2).

Procedures

This study comprised three parts corresponding to three different objectives. The first part was concentrated on the discovery and validation of several miRNAs as potential novel biomarkers of SPHS. In the second part, we conducted an integrated transcriptomic-proteomic and miRNA targets pathway enrichment analysis to reveal the significant molecular pathways relevant to leptospirosis SPHS. In the third part, we validated 10 member proteins of the resulting pathway and conducted miRNA-protein correlation analysis to study their association (Supplementary material, Section 4, S-Fig. 5).

MicroRNA

Global microRNA expression profiling

Initially, serum samples were thawed on ice and underwent cell-free total RNA extraction using the miRNeasy Serum/Plasma Kit (Qiagen in Gaithersburg, MD, USA) according to the manufacturer's protocol. Briefly, 5 volumes of QIAzol lysis reagent were added to 200 μl of serum, mixed and incubated at room temperature in 5 min. Next, 200 μl of chloroform was added and shaken vigorously for 15 s then incubated for 3 min. After centrifugation for 15 min at 12,000 g at 4 °C, the upper aqueous phase was transferred to a new collection tube and 1.5 volumes of 100% ethanol were added. The resulting sample was repeatedly transferred into an RNeasy MinElute spin column and centrifuged at ≥8000 g for 15 s. After three washes with buffers and 80% ethanol, the column was centrifuged at full speed for 5 min. Finally, the column was eluted with 14 μl Rnase-free water.

A subset of 12 serum samples (7 non-SPHS, 5 SPHS) was randomly selected for analysis with Nanostring nCounter® Human v3 miRNA Expression Assays (NanoString Technologies, Seattle, USA), which profiles the expression of 798 miRNAs simultaneously. Briefly, 3 μl of final RNA solutions from each sample were used and the experiment followed manufacturer's protocol. Then, tags ligation was followed by hybridization with the Reporter CodeSet and

Capture ProbeSet. The prepared samples were processed on the NanoString Prep Station, loaded onto the nCounter cartridge, and analyzed using the nCounter Digital Analyzer, which captured data and images across 280 fields of view. Raw counts were processed with nSolverTM software (version 4.0), adjusted by subtracting the geometric mean of negative controls, and normalized using the geometric mean of positive controls and the top 100 most highly expressed miRNAs, which were defined by the averaged counts across all samples.

MicroRNA validation by Realtime quantitative Polymerase Chain Reaction (RT-qPCR)

The quantification of miRNA candidates was carried out through RT-qPCR following a previously established protocol.[22] The process includes three main steps: polyuridylation, reverse transcription reaction, and RT-qPCR. Total RNA (7 μl) was initially polyuridylated using UTP and poly(U) polymerase. The tailing reaction mixture was incubated at 37^0 C for 10 min. cDNA molecules were then reverse transcribed using universal poly(A) stem-loop RT primers by RevertAid First Strand cDNA Synthesis Kit (Cat No. 1622, Thermo Scientific, USA).

For RT-qPCR, a miRNA-specific forward primer and a universal reverse primer were used with the StepOne Plus Real-time PCR System (Applied Biosystems, USA). The miRNA-specific forward primer's 3′-end was designed to hybridize to the cDNA molecule of the targeted miRNA, while a tail was introduced at the 5′-end to adjust the melting temperature. The SYBR Green system (Luna Universal qPCR Master Mix, Cat No. M3003, New England Biolabs, Inc., USA) was used to evaluate miRNA levels with 1 μl of template cDNA for each reaction. Primer sequences are provided in S-Table 3 (Supplemental materials). RT-qPCR reactions were conducted in duplicates with 40 cycles. The miRNA relative expression level was calculated using the $2^{-\Delta\Delta CT}$ method. Each assay was examined for distinct melting curves, and those with more than one melting temperature or within five cycle thresholds of the negative control (Ct exceeding 35) were omitted from the analysis. [23]

Accounting for hemolysis and selection of an appropriate endogenous reference for RT-qPCR quantitative analysis

To account for hemolysis, the ratio between miR-451a and miR-23a-3p was measured. [24] Since 52% of our samples had a hemolysis ratio of above 7, which suggests possible hemolysis, we searched for an appropriate endogenous reference that met two criteria: (1) highly and stably expressed across SPHS and nonSPHS samples, and (2) not prone to hemolysis. Our full approach is detailed at S-Fig. 3 (Supplementary material). Briefly, we calculated stability value using NormFinder on our nCounter® data, and intersected the miRNAs with lowest stability values with those least affected by hemolysis, referenced from the work of MacLellan et al. [23] The process revealed miR-23a-3p as an optimal option. Interestingly, this miRNA has been known for its stable expression in serum and plasma samples and were recommended as endogenous control by several studies of circulating miRNA. [25–28] When measured in our whole cohort, miR-23a-3p displayed a stable expression across SPHS and hemolysis groups (S-Table 2).

For our main analysis, relative expressions were calculated with miR-23a-3p as normalizer. We also conducted a sensitivity analysis excluding all samples with hemolysis ratio above 7 and compared the performance of our best biomarkers when normalized by miR-23a-3p and by miR-16-5p-a widely accepted normalizer given hemolysis is unlikely.[29]

Transcriptomics

We obtained a gene expression dataset from GEO Omnibus (accession ID: GSE72946) to enrich the pathway analysis. This study measured the acute phase global gene expression in whole blood samples of Brazilian leptospirosis patients, including 13 non-fatal and 3 fatal patients.[30] Of note, the three fatal cases differed with non-fatal cases by severe pulmonary involvement, including hemoptysis, acute respiratory failure and mechanical ventilation requirement, which were all suggestive of SPHS. A comparison of the patients' clinical features was demonstrated in S-Table 4 (Supplementary materials). For convenience, we labeled the two groups as non-SPHS and SPHS in this study.

Proteomics

Global protein expression data were obtained through a sequence of two experiments. Matrix-Assisted Laser Desorption/Ionization Time-of-Flight (MALDI-TOF) were performed on plasma samples to survey the peptide expression and select optimal samples for Liquid Chromatography-Tandem Mass Spectrometry (LC-MS/MS). The LC-MS/MS phase involved plasma samples from 57 non-SPHS and 19 SPHS patients. Peptides in each plasma sample were pooled and prepared for injection into an Ultimate3000 Nano/Capillary LC System (Thermo Scientific, UK) coupled to a ZenoTOF 7600 mass spectrometer (SCIEX, Framingham, MA, USA). The non-SPHS group was analyzed in six replicates and the SPHS group in three replicates (S-Fig. 6). Further details for MALDI-TOF and LC-MS/MS experiments, including data acquisition and data preprocessing, are provided in the Supplementary materials, Section 4.

Olink® proteomics for pathway proteins validation

The expression of 10 relevant proteins were measured using proximity extension assay technology (Olink® Target 96 Inflammation panel version v.3025). Briefly, the plasma samples from the same set of patients in LC-MS/MS experiments were sent to a core lab in a randomized batch. Data generation and quality control were performed with Olink® NPX Signature normalization. The expression values were in Normalized Protein Expression (NPX) unit.

Bioinformatic analysis

The expression data obtained from miRNA profiling, gene expression and LC-MS/MS proteomics followed a common analytic workflow. All expression values were log2 transformed and quantile normalized. Missing protein intensities were imputed using random forest method. [31] Differential analyses were conducted using empirical Bayes method in *limma* R package.[32] A hierarchical model was fitted with the non-SPHS group as reference to calculate moderated t-statistics, log2 fold-change (log2FC) and p-values. Multiple comparison were adjusted using false discovery rate (FDR) q-value method from *qvalue* R package, with a q-value < 0.05 considered statistically significant.[33] Principal component analysis (PCA), component loadings, and Eigencor plot were conducted using *PCAtools* R package.[34]

The validated and reviewed targets of miRNAs were obtained from MirTarBase update 2022 and TarBase-v9.0 (S-Table 5).[35,36] For pathway enrichment analysis, lists of differentially regulated genes and proteins were separately uploaded to STRING database v12.0 for protein-protein interaction (PPI) analysis, with a confidence cutoff at 0.7. The largest module from PPI analysis was selected for pathway enrichment in Cytoscape, using the Kyoto Encyclopedia of Genes and Genomes (KEGG) database. [37] An integrative gene-protein analysis was further conducted using ActivePathways R package, following its published protocol.[38] Enriched pathways were visualized using Cytoscape version 3.9.1 and the EnrichmentMap plugin, with relevant KEGG pathways created by KEGG mapping tools. [39]

The scheme for the multi-omics pathway enrichment analysis was described in the Supplemental materials (Section 4, S-Fig. 5).

Briefly, the analysis was performed initially on single-omics data then on the integrated at gene-ID level data. The resulting pathways were intersected with miRNA target-enriched pathways.

Statistical analysis

Continuous variables were described by mean and standard deviation (SD) for normally distributed data, or median and interquartile range (Q1,Q3) for skewed data. Two-sample Welch's t-test was used to compare the log10 transformed relative expression of the miRNA between two groups. Predictive values, including area under the curve (AUC) and its 95% confidence interval (CI), were obtained through Receiver Operating Characteristic (ROC) curve analysis and De Long's method using the *pROC* R package on the total sample size of 168 patients.[40]

Multivariable logistic regression was employed to assess the robustness of the miRNAs when adjusting for potential confounders, including age, sex, comorbidity, smoking status, recruitment site and cohort. While age and sex have been widely recognized as confounders of circulating miRNA expression, existing evidence also suggested the effect of comorbidity, like diabetes and hypertension, on serum miRNAs.[41,42] The effect of smoking status on circulating miRNA expression is controversial, however, considering its potential effects on lung status, we included it in the analysis.[23,43] We also adjusted for the effect of recruitment sites since difference in local practice might have an effect on the quantification result of the miRNAs.

Bayesian model averaging algorithm from *BMA* R package was used to suggest the most parsimonious combination of miRNA-miRNA or miRNA-protein for predictive logistic regression model.[44] Correlations between miRNA and protein expressions were performed using a non-parametric test (Spearman's test). Of note, only 10 out of 96 proteins in Olink® panel were reported since we specifically focus on the most important pathway suggested by multi-omics analysis. This maintained a hypothesis-driven approach and avoided unnecessary multiple testing. Multivariable linear regression and likelihood ratio test were used to compare model with and without interaction term.

To facilitate the interpretation of miRNA biomarkers in practice, three different cut-offs for different usage scenarios were introduced. They included the overall optimal cut-off following Youden index method (maximizing the sum of sensitivity and specificity), the sensitivity-prioritized cut-off for use as a screening tool (controlling sensitivity at 99% while maximizing specificity) and the specificity-prioritized for use as a rule-in test to support treatment decision (controlling specificity at 99% while maximizing sensitivity).

To test whether the inclusion of microRNA biomarkers improves discrimination and reclassification for SPHS, a previously developed and validated clinical model for SPHS prediction including shock at admission, respiratory rate, Glasgow score, serum potassium and serum creatinine was used as the baseline model, and compared to model with microRNA biomarkers.[9] Improvement in discriminatory performance was tested using two ROC curves test function in pROC R package (De Long's method). Reclassification tabulation was performed with *PredictABEL* R package to calculate net reclassification index (NRI) and Integrated Discrimination Index (IDI). Cut-off for reclassification analysis was selected at two intervals: 0–50% and 50–100%, according to the original publication of the clinical model.[9] All computational analyses were conducted in Rstudio version 4.3.1.

Role of the funding source

The funding source had no active role in study design, data collection, data analysis and interpretation, manuscript preparation and publication.

Results

Clinical characteristics

From the biorepository and available clinical data, we identified 28 leptospirosis patients with clinical features of SPHS and randomly selected 140 non-SPHS patients, following the flowchart in Fig. 1. Overall, patients in both groups had comparable ages (median of 47 and 51.5 years for non-SPHS and SPHS, respectively) and a predominance of male sex. All patients had a history of fever and were admitted during the febrile phase, with recruitment occurring at a similar stage of illness, a median of three days since fever onset (Table 1).

On recruitment day, SPHS patients exhibited more severe clinical features compared to non-SPHS patients. The SPHS group had significantly lower systolic blood pressure (mean of 90.6 ± 16.5 mmHg) compared to the non-SPHS group (115 ± 23.1 mmHg). Jaundice was observed in 21.4% of SPHS patients versus 8.6% in the non-SPHS group. The SPHS group also showed lower hematocrit levels, platelet counts, higher total bilirubin levels, and lower albumin levels. The Sequential Organ Failure Assessment (SOFA) score and the number of organs involved were substantially higher in the SPHS group. While both groups had similar rates of positive MAT for leptospirosis, leptospiremia was higher in the SPHS group (96.4%) compared to the non-SPHS group (83.6%). During hospitalization, eight SPHS patients and three non-SPHS patients died (Table 1).

Discovery and validation of miRNA biomarkers

Global miRNA profiling revealed a total of 81 differentially expressed miRNAs, including 13 up-regulated and 68 down-regulated miRNAs (Fig. 2A). These miRNAs exhibited clear clustering in the heatmap visualization (Fig. 2B). We randomly selected seven miRNAs (hsa-miR-5010–3p, miR-147b-3p, hsa-miR-362-3p, hsa-miR-502-5p, hsa-miR-3131, hsa-miR-548ai and hsa-miR-224-5p) among the most differentially expressed molecules for validation.

In validation phase, three miRNAs exhibited significantly different expressions that were consistent with nCounter results, including the upregulation of miR-5010–3p, miR-147b-3p and the downregulation of miR-548ai. MiR-3131 and miR-224–5p were significantly expressed with contrast direction compared to nCounter experiment (Fig. 2C).

For predictive performance, miR-5010–3p and miR-147b-3p had the most optimal AUC values, at 0.76 (95% CI: 0.67–0.85) and 0.70 (95% CI: 0.58–0.81) (Fig. 3A). Other miRNAs, such as miR-548ai, miR-3131, and miR-224–5p, also demonstrated significant discriminatory ability for SPHS patients with lower AUC values (Fig. 3A). Among these, miR-5010–3p and miR-147b-3p displayed noticeable positive correlations with clinical markers of acute blood loss (hematocrit level), bleeding risk (platelet counts), and clinical severity (SOFA score and the number of organ involvements) (Fig. 3B). We thus focused on these two for further subgroup analysis. More importantly, the performance of miR-5010–3p and miR-147b-3p remained significant in patients tested before chest X-ray shadows appeared, at an AUC of 0.74 (95% CI: 0.63–0.84) and 0.70 (95% CI: 0.59–0.81), respectively. In patients recruited on day 2 of fever or earlier, both miRNAs showed increased AUC values, at 0.82, (95% CI: 0.66–0.94) and 0.84 (95% CI: 0.71–0.96), respectively (Fig. 3C). These results suggested early changes of the miRNAs in the disease course and thus suitable for use as clinical biomarker. These predictive estimates remained robust when adjusted for potential confounders such as age, sex, diabetes, hypertension, smoking status, recruitment sites or cohorts (S-Table 6).

Sensitivity analysis on samples with hemolysis ratio < 7 revealed AUC values of miR-5010–3p and miR-147b-3p that were comparable to those from the whole cohort, at 0.76 (95% CI: 0.63–0.89) and 0.66 (95% CI: 0.50–0.79) respectively (S-Fig. 4). Notably, the AUC values

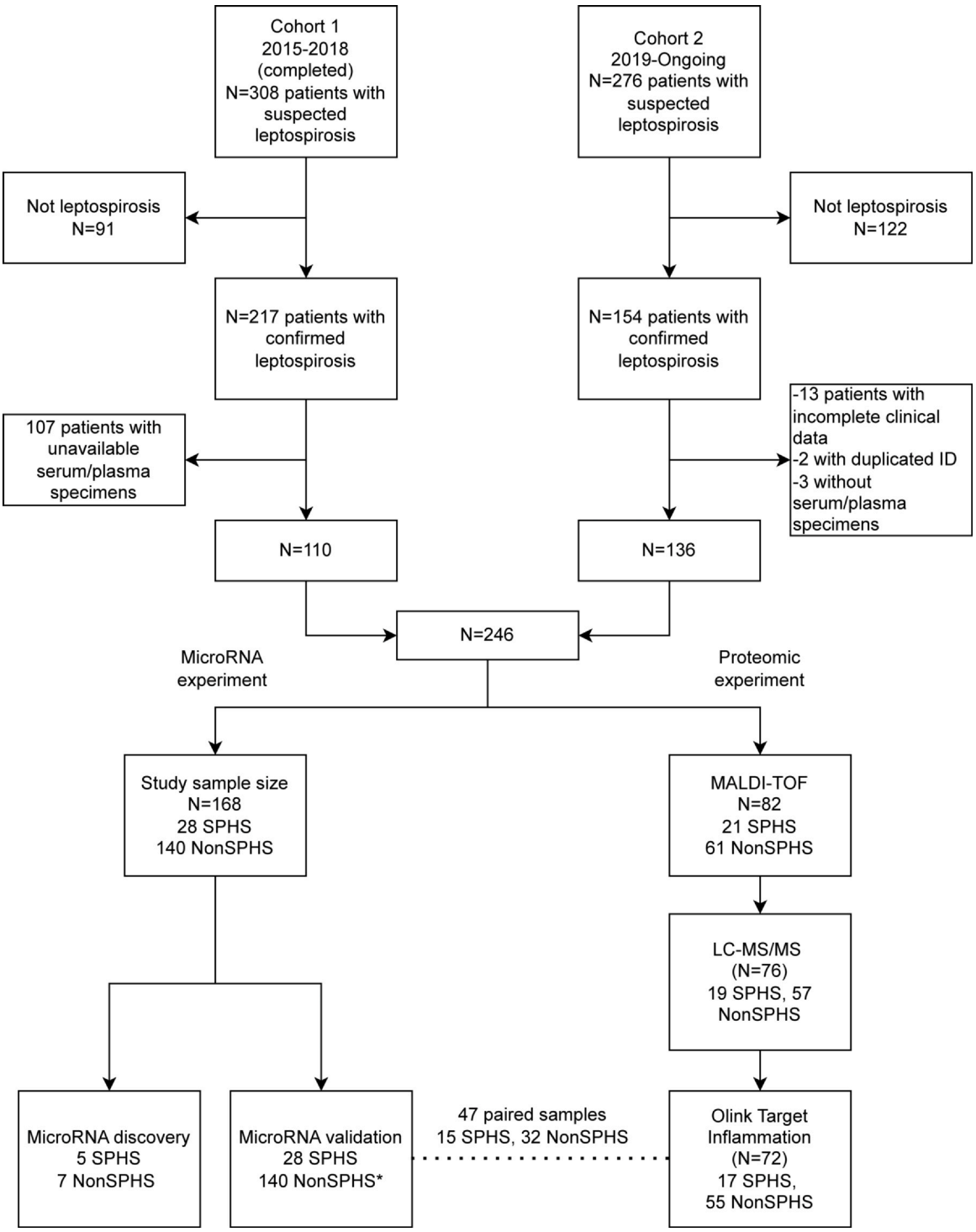

Fig. 1. The study flowchart. *One non-SPHS patient was initially included in the discovery set. However, due to specimen running out, the patient was replaced by another non-SPHS patient for the validation set. SPHS: severe pulmonary hemorrhagic syndrome.

were also similar when compared between miR-23a-3p and miR-16–5p normalizers (S-Fig. 4). Also, the relative expressions of the two miRNAs when normalized to miR-23a-3p showed strong positive correlation with those normalized to miR-16–5p (S-Fig. 4). These analyses indicate that the significant performance of these two miRNA biomarkers was not biased by hemolysis.

At their optimal cut-off points determined by Youden method, miR-5010–3p demonstrated a sensitivity of 0.77 (95% CI: 0.70–0.84) and a sensitivity of 0.68 (95% CI: 0.50–0.86), whereas the corresponding indices for miR-147b-3p are 0.61 (95% CI: 0.42–0.79) and 0.74 (95% CI: 0.66–0.80), respectively. When used as screening tool at lower cut-offs, their sensitivity can be as high as 100%, with a trade-off for lower sensitivity, at 0.26 (95% CI: 0.19–0.34) for miR-5010–3p and at 0.20 (95% CI: 0.13–0.27) for miR-147b-3p. Conversely, when used as a rule-in test, the two miRNAs specificity can be as high as 99% with a decreasing sensitivity (Table 2).

The potential of combining microRNA to improve performance was examined. BMA algorithm suggested some different sets of miRNAs, including two-miRNA, three-miRNA and four-miRNA models (Figure D). The two-miRNA model incorporating miR-5010–3p and miR-548ai

Table 1
Baseline characteristics of the patients included in this study.

	Discovery set (N=12)			Validation set (N=168)		
	Non-SPHS (n = 7)	SPHS (n = 5)	Overall (n = 12)	Non-SPHS (n = 140)	SPHS (n = 28)	Overall (n = 168)
Age (years), Median [Q1,Q3]	54.0 [44.5,58.5]	30.0 [28.0,66.0]	51.5 [36.8,61.0]	47.0 [37.0,61.0]	51.5 [29.5,62.8]	48.0 [35.8,61.0]
Male sex, n(%)	6 (85.7)	5 (100)	11 (91.7)	116 (82.9)	25 (89.3)	141 (83.9)
BMI (Kg/m^2, Mean (SD)	24.6 (5.31)	24.2 (4.03)	24.5 (4.73)	22.5 (3.93)	22.3 (3.49)	22.5 (3.87)
Diabetes, n(%)	1 (14.3)	0 (0)	1 (8.3)	4 (2.9)	0 (0)	4 (2.4)
Hypertension, n(%)	1 (14.3)	0 (0)	1 (8.3)	11 (7.9)	2 (7.1)	13 (7.7)
Alcoholism, n(%)	7 (100)	5 (100)	12 (100)	5 (3.6)	2 (7.1)	7 (4.2)
Smoking, n(%)	3 (42.9)	2 (40.0)	5 (41.7)	71 (50.7)	13 (46.4)	84 (50.0)
Days of illness (days) Median [Q1,Q3]	3 [1,3]	3 [0,3]	3 [1,3]	3 [1.75,4]	3 [2.75,4]	3 [2,4]
Clinical manifestation at specimen collection						
Temperature (^{0}C) Mean (SD)	38.7 (1.38)	37.6 (1.66)	38.2 (1.54)	38.4 (1.21)	37.8 (0.987)	38.3 (1.19)
Systolic blood pressure (mmHg)						
Mean (SD)	122 (15.5)	86.6 (22.5)	107 (25.3)	115 (23.1)	90.6 (16.5)	111 (23.9)
Diastolic blood pressure (mmHg)						
Mean (SD)	68.9 (13.6)	50.6 (17.8)	61.3 (17.5)	66.4 (11.5)	57.0 (15.9)	64.8 (12.8)
Hemoptysis, n(%)	0 (0)	2 (40.0)	2 (16.7)	0 (0)	11 (38.3)	11 (6.5)
Jaundice, n(%)	0 (0)	1 (20.0)	1 (8.3)	12 (8.6)	6 (21.4)	18 (10.7)
Hemoglobin (g/dL) Median [Q1,Q3]	12.7 [10.8,12.9]	8.60 [8.40,12.5]	11.7 [8.55,12.7]	12.2 [11.1,13.3]	11.2 [9.13,12.5]	12.1 [10.8,13.2]
Hematocrit (%) Median [Q1,Q3]	38.0 [34.0,39.3]	26.3 [24.9,38.0]	36.0 [26.1,39.2]	38.0 [34.0,40.8]	32.6 [26.3,36.1]	37.0 [33.2,40.0]
Leukocytes (1000/uL) Median [Q1,Q3]	13.2 [10.8,15.3]	8.7 [8.6,12.2]	12.3 [8.7,15.1	10 [7.5,12.6]	9.9 [6.4,12.9]	10 [7.1,12.6]
% Neutrophils Median [Q1,Q3]	80.0 [75.0,85.5]	84.0 [82.0,91.0]	82.5 [79.3,88.7]	83.0 [73.0,87.9]	86.0 [82.5,90.9]	84.0 [74.9,88.0]
% Lymphocytes Median [Q1,Q3]	11.0 [7.00,18.4]	7.10 [6.00,9.00]	9.50 [5.50,12.0]	9.95 [6.80,17.0]	7.05 [4.00,9.25]	9.00 [6.00,15.0]
Platelets (1000/uL) Median [Q1,Q3]	188 [117,244]	54 [19,69]	85 [50.8,188]	139 [82.3,199]	37.5 [22.8,60]	109 [53.5,190]
Blood urea nitrogen (mg/dL) Median [Q1,Q3]	16.5 [13.9,44.0]	26.0 [24.0,36.3]	24.0 [14.6,44.7]	16.9 [13.0,26.0]	36.3 [25.0,52.4]	19.7 [13.9,31.3]
Serum creatinin (mg/dL) Median [Q1, Q3]	1.05 [0.915,3.55]	2.00 [1.22,3.04]	1.61 [1.03,3.33]	1.20 [0.930,1.60]	2.23 [1.63,4.28]	1.30 [0.960,1.96]
Serum total bilirubin (mg/dL) Median [Q1,Q3]	0.800 [0.700,1.19]	2.40 [1.60,3.01]	1.19 [0.700,2.55]	1.10 [0.700,2.10]	3.11 [1.28,7.68]	1.20 [0.700,2.40]
Serum SGOT (UI/L) Median [Q1,Q3]	39.0 [31.5,57.5]	98.0 [50.0,101]	44.5 [37.8,98.8]	50.0 [32.0,87.5]	94.0 [54.0,141]	53.5 [34.0,104]
Serum SGPT (UI/L) Median [Q1,Q3]	36.0 [30.5,56.5]	32.0 [32.0,78.0]	34.0 [31.3,75.8]	40.5 [25.8,90.0]	44.0 [32.0,65.0]	43.0 [27.0,81.0]
Serum albumin (g/dL) Median [Q1,Q3]	3.25 [2.95,3.55]	2.50 [2.20,3.20]	3.10 [2.65,3.50]	3.50 [3.11,3.88]	2.77 [2.30,3.13]	3.40 [2.99,3.80]
Serum sodium (meq/L) Mean (SD)	137 (3.51)	138 (3.27)	137 (3.27)	135 (4.59)	134 (4.90)	134 (4.64)
Serum potassium (meq/L) Median [Q1,Q3]	3.67 [3.50,3.95]	3.60 [3.60,4.30]	3.64 [3.55,4.23]	3.60 [3.30,3.92]	3.60 [3.35,3.98]	3.60 [3.30,3.93]
Serum chloride (meq/L) Mean (SD)	99.9 (4.34)	104 (10.9)	102 (7.61)	97.9 (8.10)	99.1 (6.51)	98.1 (7.84)
Serum bicarbonate (meq/L)						
Mean (SD)	24.9 (3.11)	19.3 (7.02)	22.6 (5.60)	24.6 (7.80)	19.5 (5.26)	23.7 (7.66)
SOFA score Median [Q1,Q3]	0 [0,5]	10 [8,14]	6 [0,8.5]	2 [1,4]	12.5 [10.8,14.3]	3 [1,6]
Number of organ involvement						
Median [Q1,Q3]	0 [0,1.5]	4 [2,4]	2 [0,3.25]	1 [0,1]	4 [3,5]	1 [0,2]
Leptospiral diagnostic features						
Positive MAT, n (%)	1 (14.3)	1 (20.0)	2 (16.7)	47 (33.6)	10 (35.7)	57 (33.9)
Leptospiremia[a], n (%)	7 (100)	5 (100)	12 (100)	117 (83.6)	27 (96.4)	144 (85.7)
Patient outcomes						
ICU admission, n (%)	1 (14.3)	4 (80.0)	5 (41.2)	7 (5.0)	24 (85.7)	31 (18.5)
Hospital mortality, n (%)	0 (0)	1 (20.0)	1 (8.3)	3 (2.1)	8 (28.6)	11 (6.5)
90-day mortality, n (%)	0 (0)	1 (20.0)	1 (8.3)	4 (2.9)	9 (32.1)	13 (7.7)

[a] Leptospiremia was defined as either positive blood qPCR for pathogenic Leptospira spp. or a positive blood culture.

achieved an AUC value of 0.85 (95% CI: 0.76–0.93), while adding miR-224–5p and miR-3131 further extend the AUC values to as high as 0.89 (95% CI: 0.80–0.96). Interestingly, these combinations also improve sensitivity and specificity at three different usage scenarios as compared to single miRNA (Table 2).

The benefits of integrating novel miRNA biomarkers to improve clinical model predictions were illustrated. A baseline clinical model involving five baseline parameters (respiratory rate, Glasgow score, serum creatinine, serum potassium and shock at admission) had an AUC of 0.87 (95% CI: 0.8–0.94). When adding miR-5010–3p or miR-147b-3p, the AUC values significantly increased to 0.92 (95% CI: 0.87–0.97), suggesting an improved discriminatory performance. Furthermore, the updated model leads to a significant reclassification of leptospirosis with and without SPHS. The net reclassification index (NRI) is 0.9 (0.545–1.255), p-value < 0.0001 and integrated discrimination index (IDI) is 0.083 (0.037–0.13), p-value < 0.0001 for miR-5010–3p (Fig. 3G). These results strongly suggest that novel miRNA biomarkers are useful for extending and updating existing predictive models.

Multi-omics pathway enrichment analysis

To understand the role of the miRNA biomarkers, we performed pathway analysis leveraging both gene expression and protein expression data, the two omics layers that are most relevant to miRNA mechanism of action. Clinically, patients in both types of omics data were all in febrile phase, although transcriptomics patients tended to be younger overall (S-Table 4).

Gene expression analysis unveiled 629 up-regulated and 698 down-regulated genes (Fig. 4A). Heatmap visualization highlighted distinct clusters among the top DE genes (Fig. 4B). Proteomic analysis revealed 496 up-regulated and 679 down-regulated protein groups (Fig. 4C), with similar clustering on heatmap plot (Fig. 4D). Many gene-protein pairs associated with the host immune response exhibited similar directional changes, such as ACOD1, BCL2A1, IL1R1, TLR4, and HIVEP3. However, others showed an opposite pattern, including DEFA4, IL18R1, TLR8, and certain immunoglobulins (Fig. 4E).

PPI analysis revealed a large, connected module per each gene/protein list (S-Fig. 7), with CTNNB1, IL10, IL6, CD74, FN1 appearing as high degree nodes. Single-omics pathway enrichment analysis revealed numerous significant pathways related to signal transduction, the immune system, and infectious diseases. Up-regulated genes and proteins were associated with a greater number of overlapping pathways, particularly those involved in inflammatory responses such as NF-kappa B, PI3K-Akt, and TNF signaling pathways. In contrast, downregulated genes and proteins were enriched in fewer

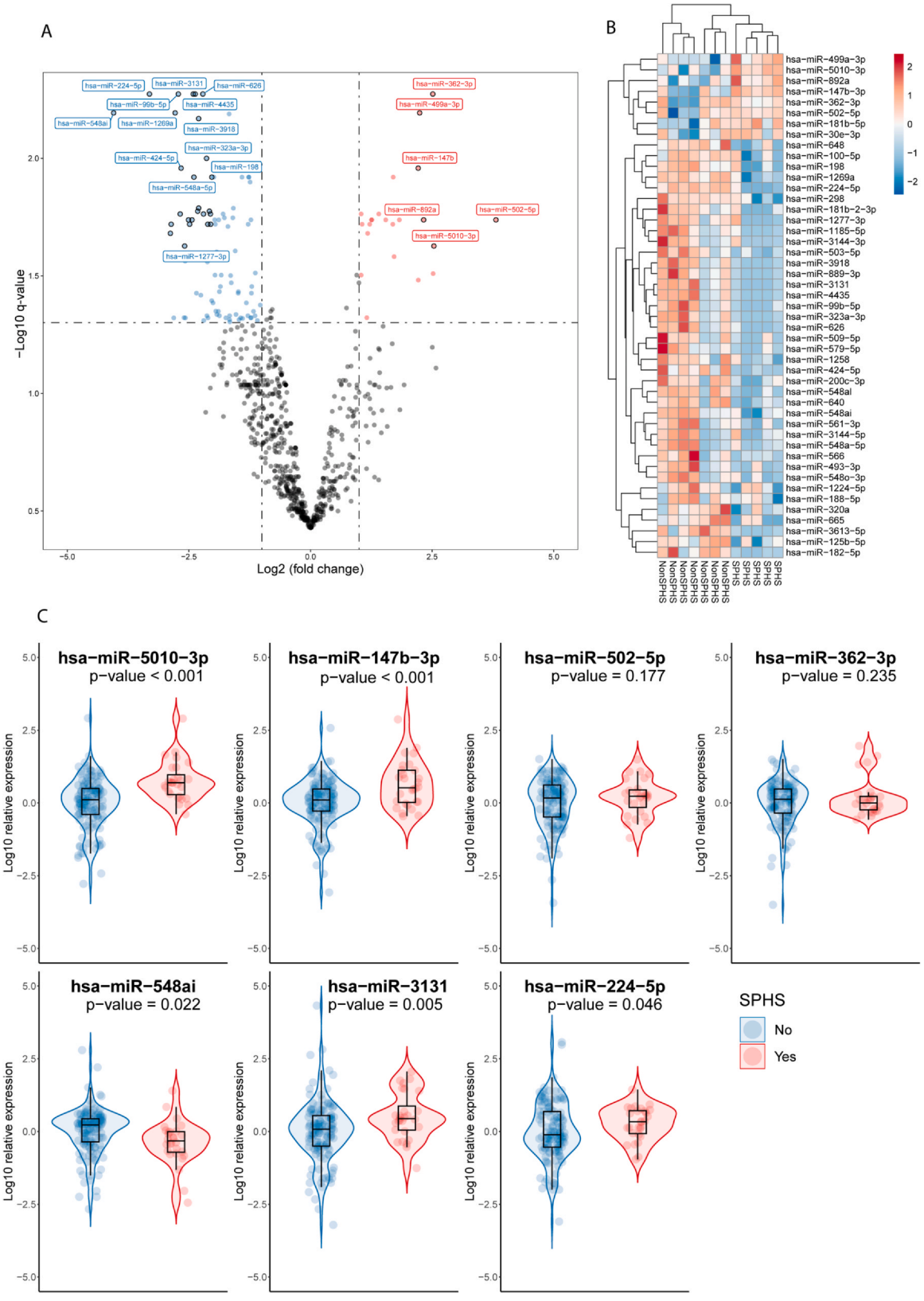

Fig. 2. Discovery and validation of serum microRNAs. (A) Volcano plot showing the log2 fold-change in relation to -log10 q-values of the miRNAs expression levels. The log2 fold-change and q-values were calculated using the empirical Bayes method in *limma* and *qvalue* R packages (moderated t-statistics). The red and blue circles represent up- and down-regulated miRNAs, respectively. The miRNAs with lowest q-values and largest fold-changes were labeled. (B) Heatmap showing the distance clustering of the top miRNAs, using Euclidean method incorporated in *pheatmap* R package. The color gradient describes the row-normalized z-score. (C) Violin plots comparing relative expressions of the seven miRNAs. The relative expression was calculated following the $2^{-\Delta\Delta CT}$ method, with miR-16–5p as reference. The dots represent a log10 relative expression of a miRNA for one patient. The p-values were calculated using two-sample Welch's t-test. SPHS: severe pulmonary hemorrhagic syndrome.

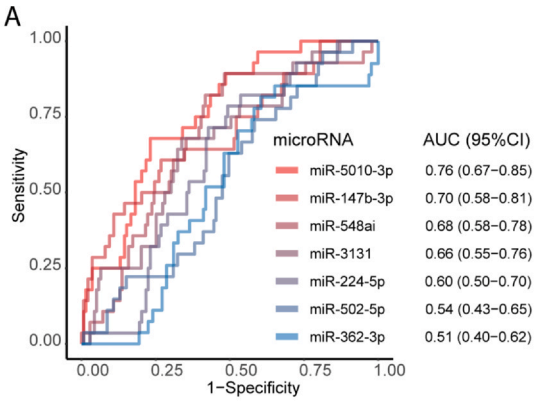

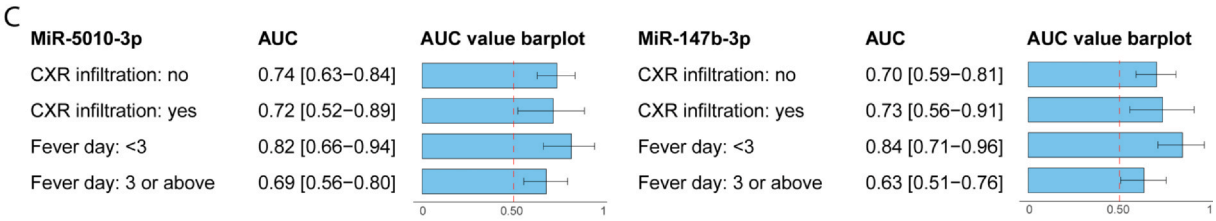

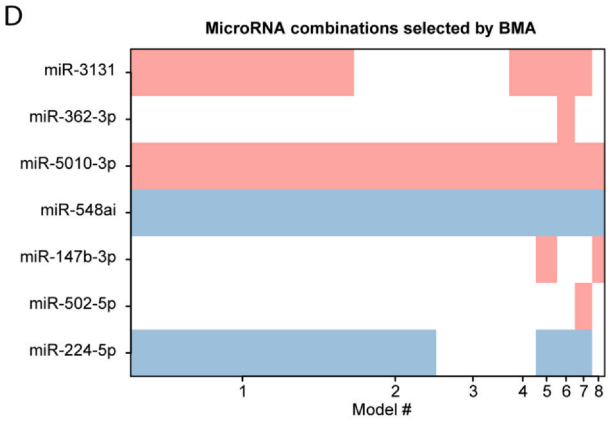

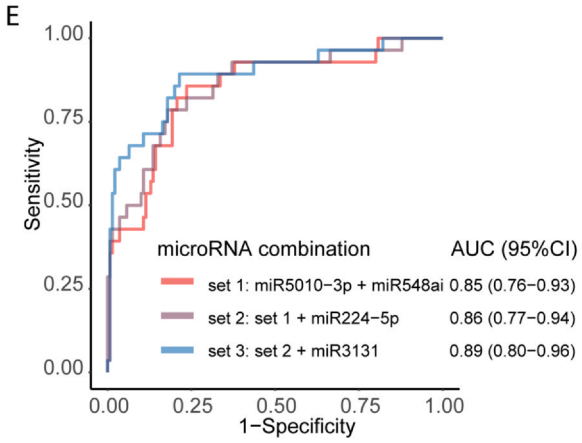

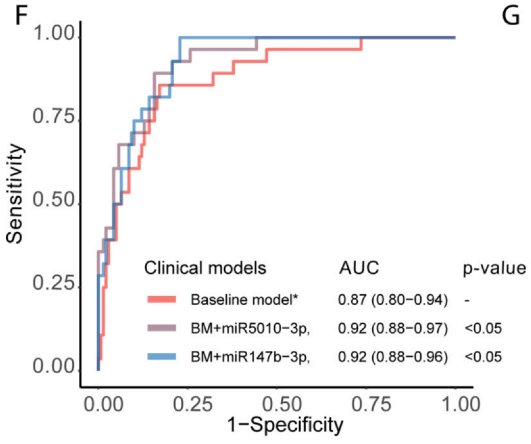

*Baseline model: Respiratory rate, Glasgow <15, serum creatinin, serum potassium, shock

G

Reclassification		Clinical model + miR-5010-3p			Clinical model + miR-147b-3p		
	Risk level	0–0.5	0.5–1	%RC	0–0.5	0.5–1	%RC
Clinical model							
NonSPHS	0–0.5	131	3	2%	132	2	1%
	0.5–1	3	3	50%	2	4	33%
SPHS	0–0.5	11	4	27%	11	4	27%
	0.5–1	1	12	8%	3	10	23%
Combined	0–0.5	142	7	5%	143	6	4%
	0.5–1	4	15	21%	5	14	26%
NRI (Continuous)		0.9 [0.545–1.255] ;			0.814 [0.438–1.190] ;		
95% CI; p-value		p-value: <0.0001			p-value: <0.0001		
IDI		0.083 [0.037–0.13] ;			0.067 [0.005–0.129] ;		
95% CI; p-value		p-value: <0.0001			p value: 0.033		

(caption on next page)

Fig. 3. MiRNAs as biomarkers of leptospirosis SPHS. (A) Receiver Operating Characteristics (ROC) curve analyses. The curves are colored by the seven miRNAs of interest. Area under the curve (AUC) values and 95% CIs were calculated using pROC R package, using the log10 relative expression of the corresponding miRNAs against their SPHS classification. (B) Correlation matrix between miRNAs and clinical indicators of acute blood loss and severity. Correlations between miRNAs and clinical features were performed using Spearman's test. The gradient indicates correlation coefficients, with positive value in red and negative in blue. The dot size represents the magnitude of the value. The numbers inside the dots represent the correlation coefficients. The asterisk indicate a significant correlation. (C) AUC values in relation to chest radiographs (CXR) and fever day. For this figure, SPHS patients were classified as already having abnormality on chest radiographs (n=22) or not (n=6) (at blood collection) and compared with non-SPHS patients (n=140). For fever day, we divided the 168 patients into two groups (day 2 or earlier and day 3 or above), each comprised 66 (non-SPHS = 59, SPHS = 7), 72 (non-SPHS = 81, SPHS = 21) patients, respectively. AUC values and 95% CIs were calculated and plotted as previous analyses. (D) MiRNA combination selected by BMA algorithm. Each row indicates whether a miRNA should be included (colored in red or blue), or not (white color). The red bars mean a positive coefficient in the logistic regression model, whereas blue bars mean negative. It could be observed that the first model includes miR-3131, miR-5010–3p, miR-548ai and miR-224–5p; whereas the second model includes miR-5010–3p, miR-548ai and miR-224–5p; and so on. (E) ROC curve analyses of the miRNA models. The ROC curve and AUC values were first calculated by fitting a miRNA model with logistic regression with SPHS group as outcome variables. After that, the predict function was used to calculate the individual risk (probability value) of each patient when evaluating by the miRNA model. The risk was then used to calculate the AUC and ROC curve following method in figure A. (F) Novel miRNA biomarkers enhanced clinical model prediction. The baseline model included five clinical parameters: respiratory rate, Glasgow < 15, serum creatinine, serum potassium and shock at admission (Marotto et al.). The original equation of the baseline model was used to calculate the individual risk, then the risk was used to calculate AUC values and ROC curve as in figure A. MiRNA was added to the model and followed the same process to draw the ROC curves. The baseline model and the model with miRNA were compared using ROC test function in pROC R package, following De Long's method. (G) Reclassification table. The table was created using the predictABLE R package, with the clinical model as baseline and model with miRNA as updated model. The risk cutoff was defined at 50% based on the original paper of the clinical model. The colored cells indicated consisted of classification between baseline and updated model. SOFA: Sequential Organ Failure Assessment. RC: Reclassification. NRI: net reclassification index. IDI: Integrated Discrimination Index. AUC: area under the curve. ROC: receiver operating characteristics.

Table 2
Sensitivity and specificity at optimal cut-off points of the microRNAs.

	Maximized sensitivity+specificity (Youden's method)	Sensitivity controlled at 99%	Specificity controlled at 99%
miR-5010-3p			
Cut-off (log10 relative expression)	0.518	−0.390	1.390
Sensitivity (95%CI)	0.68 (0.50–0.86)	1 (1–1)	0.18 (0.04–0.32)
Specificity (95%CI)	0.77 (0.70–0.84)	0.26 (0.19–0.34)	0.99 (0.96–1)
miR-147b-3p			
Cut-off (log10 relative expression)	0.433	−0.484	1.425
Sensitivity (95%CI)	0.61 (0.42–0.79)	1 (1–1)	0.14 (0.03–0.29)
Specificity (95%CI)	0.74 (0.66–0.80)	0.20 (0.13–0.27)	0.99 (0.96–1)
Combination 1: 5010-3p+548ai			
Cut-off (predicted probability)	0.223	0.020	0.413
Sensitivity (95%CI)	0.86 (0.71–0.96)	1 (1–1)	0.39 (0.21–0.57)
Specificity (95%CI)	0.76 (0.69–0.83)	0.20 (0.14–0.27)	0.99 (0.98–1)
Combination 2: 5010-3p+548ai+224-5p			
Cut-off (predicted probability)	0.186	0.013	0.423
Sensitivity (95%CI)	0.79 (0.61–0.93)	1 (1–1)	0.42 (0.25–0.61)
Specificity (95%CI)	0.82 (0.77–0.88)	0.10 (0.05–0.15)	0.99 (0.98–1)

pathways with less overlap. Interestingly, many pathways belonging to the cell community and motility, infectious disease and signal transduction category overlapped with those enriched by miRNA targets (Fig. 5A). There were 17 pathways that appeared in up-regulated genes, proteins and the two miRNAs (Fig. 5B).

To further retain the most relevant pathways, integrated analysis incorporating transcriptomic and proteomic data at the gene ID level was conducted, which yielded nine pathways. Among them, three emerged through combined-omics enrichment, with the TNF signaling pathway standing out as the most significant, evidenced by the lowest adjusted p-value (S-Table 7). Notably, TNF signaling pathway also had its member genes targeted by the two miRNA biomarkers (Fig. 5C). The ranked list of genes and protein's view revealed that CASP10, the target of miR-5010–3p, and AKT2 and PGAM5, the target of miR-147b-3p, showed consistent down-regulation in both layers (Fig. 5D and S-Fig. 8). These signals suggested that TNF signaling pathway might be an important host response mechanism in SPHS.

TNF signaling pathway proteins and miRNA biomarkers

The significance of TNF signaling pathway proteins was confirmed by Olink® proteomics results, with seven out of ten proteins showing significant differences, especially the upregulation of TNF in SPHS patients (Fig. 6A). SPHS and non-SPHS patients formed two clusters based on the first two principal components (PC) (Fig. 6B), indicating distinct global expression profiles of TNF signaling pathway proteins between the two phenotypes.

In 47 patients with paired measurements of miRNA and TNF signaling proteins, correlation analysis showed a similar pattern between miR-5010–3p or miR-147b-3p and the proteins. Significant positive correlations were found between miR-5010–3p and TNF, CCL20, while significant negative correlations were with CASP8, LTA, and CXCL5 (Fig. 7A). For miR-147b-3p, only the correlation with CCL20 reached significant threshold (Fig. 7A). Further analysis revealed that the correlation between miR-147b-3p and its target, LIF, was modulated by TNF level, indicated by a significant miR-147b-3p–TNF interaction term (p-interact < 0.05 and p-value adjusted for interaction term < 0.05) with different regression slopes based on TNF levels (Fig. 7B, upper and lower left). In contrast, no significant interaction term was found for the miR-5010–3p and CASP8 or CXCL5 pair (Fig. 7B, upper and lower right, p.interact > 0.05).

Eigencor plot showed strong correlations between the PC1 and PC2 of the TNF signaling pathway profile and clinical severity parameters, such as SOFA (r=0.72) and hematocrit levels (r=−0.39). Meanwhile, PC1 and PC5 significantly correlated with miR-5010–3p (r=0.28 and −0.26, respectively). PC1 was primarily influenced by IL6 and CXCL5, while PC5 was explained by CASP8, TNF and CCL20 (Fig. 7C). This evidence suggested correlations between TNF signaling pathway proteins and miR-5010–3p, though these were less dominant than the correlations between the cytokines and clinical severity.

The expression patterns of TNF signaling pathway proteins and miRNA biomarkers enhanced the characterization of SPHS patients. In Fig. 8A, two clusters emerged: the first included miR-5010–3p, miR-147b-3p, CSF1, IL18R1, LIF, CCL20, TNF, and IL6, while the second included CASP8, LTA, CXCL1, and CXCL5. Most SPHS patients showed upregulation of the first cluster and downregulation of the second,

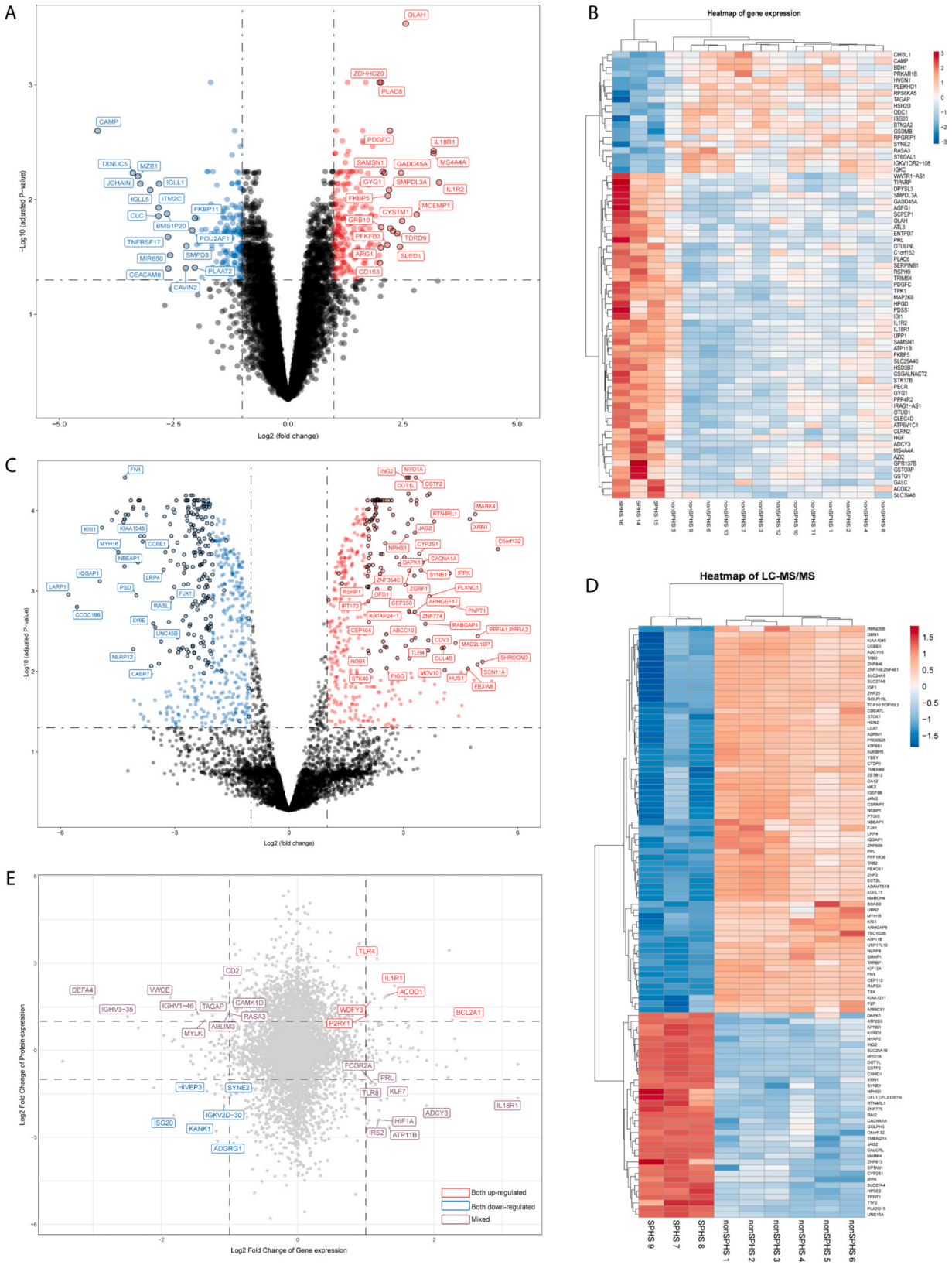

Fig. 4. Global transcriptomics and proteomics profiling. (A) and (C) Volcano plots showing the log2 fold-change in relation to -log10 q-values of the miRNAs. The log2 fold-change and q-values were calculated using the empirical Bayes method in *limma* and *qvalue* R packages (moderated t-statistic). The red and blue circles represent up- and down-regulated genes/proteins, respectively. The miRNAs with lowest q-values and largest fold-changes were labeled. (B) and (D) Heatmaps showing the distance clustering of the top genes/proteins, using Euclidean method incorporated in *pheatmap* R package. The color gradient describes the row-normalized z-score. (E) Conjoint plot showing the consistency between the log fold-change of the transcriptomics and proteomics data. The red dots represent consistently up-regulated pairs, blue dots represent consistently down-regulated pairs, purple dots represent inconsistent pairs. Only selected gene/protein symbols were labeled.

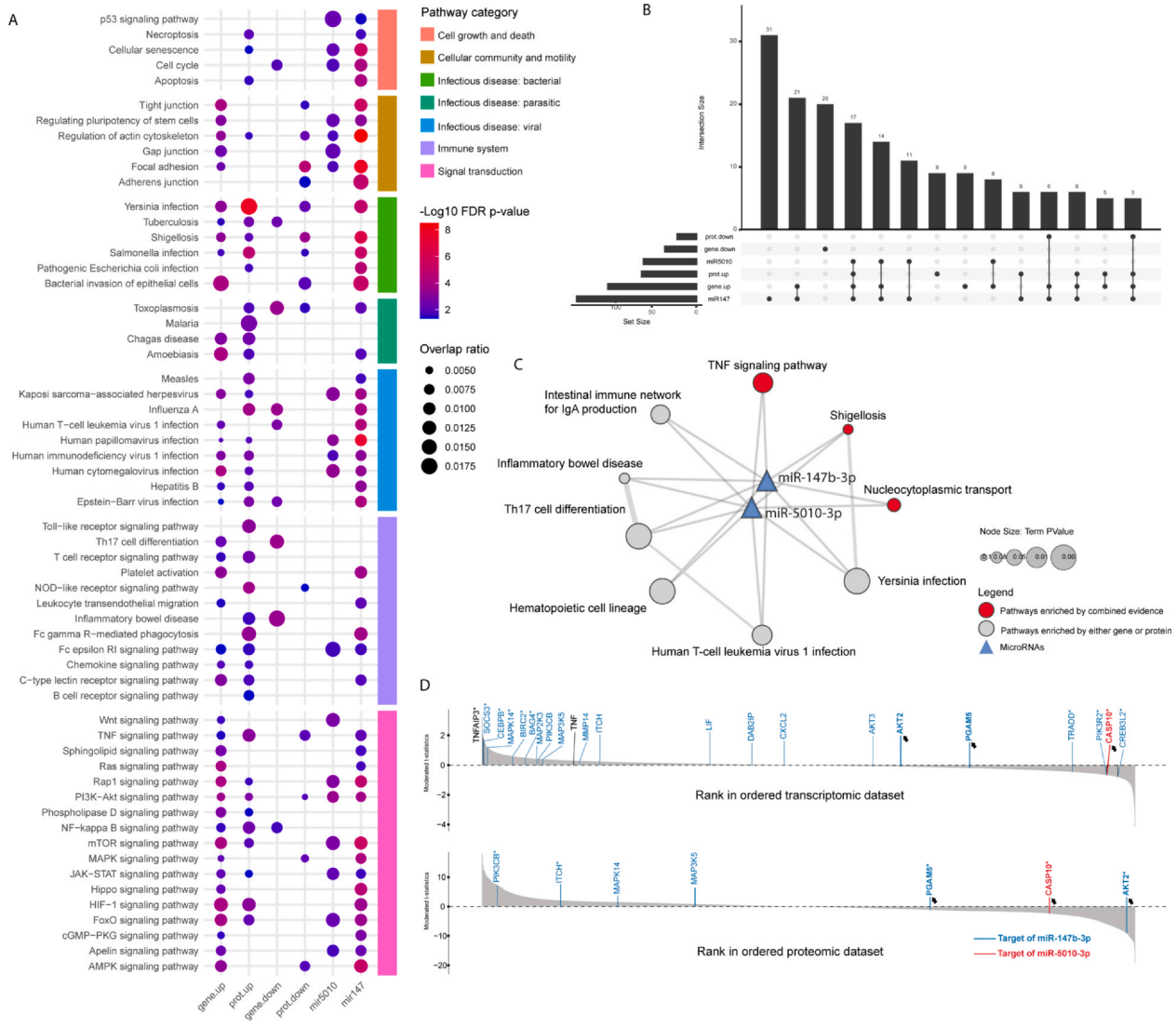

Fig. 5. Multi-omics pathway enrichment analysis. (A) Dot plots showing the significantly enriched KEGG pathway terms. Y-axis displays the selected pathway terms and x-axis indicates the types of molecular sets subjected to enrichment analyses. The dot size corresponds to the overlap ratio, which is calculated by dividing the proportion of overlap (number of molecules overlapped/total number of genes in the term) for the set size. The dots are colored by the -log10 adjusted p-values, spanning from blue (larger p-value) to red (smaller p-value). The terms on y-axis are grouped according to their KEGG category, which is annotated by colored bars. The complete enrichment results are provided in the Supplementary materials (Supplement.KEGG.enrich.results.xlsx). (B) Upset plot showing the intersections between the enrichment results. The six rows at the bottom represent the six types of molecule sets. The dots and lines represent different scenarios of intersection between the enriched terms of the sets. Black and gray dots indicate intersected and not intersected, respectively. The vertical bars at the top represent intersection size. The horizontal bars indicate the set size. (C) Enrichment map showing the link between miRNAs biomarkers and the significant pathways from Activepathways analysis. Dot size corresponds to the p-value of the pathway terms, while lines represent shared genes between the terms and miRNA targets. (D) Distribution of microRNA targets in transcriptomic and proteomic data. The gray bands represent the moderated t-statistics of the molecules in transcriptomic and proteomic data, ordered by their magnitude. The red and blue lines indicate the targets of miR-5010–3p and miR-147b-3p respectively. The asterisks indicate significant differences. Notice the consistent down-regulation of some miRNA targets in both layers (black arrows).

with non-SPHS and low SOFA score patients showing the opposite pattern (Fig. 8A). Single proteins discriminated SPHS with AUC values of 0.86 (CXCL5), 0.78 (CCL20), 0.74 (IL6), and 0.72 (TNF), though these were generally less effective compared to miR-5010–3p (0.89). Combination of cytokines and miRNA biomarkers, as indicated by the BMA algorithm, improved the performance. For example, combining miR-5010–3p, CXCL5, and IL6 increased the AUC to 0.98 (Fig. 8B). These findings suggest the potential for a biomarker panel, which should be confirmed in future studies with larger sample sizes.

Discussion

In this study, we discovered and validated miR-5010–3p and miR-147b-3p as novel biomarkers for SPHS in leptospirosis patients. These miRNAs had good performance that was robust for the potential confounders and exhibited early changes in the acute phase of the disease. Integration of the novel microRNA biomarkers appears to significantly enhance the performance of clinical model and improve reclassification. Using multi-omics pathway enrichment approach, TNF signaling pathway was identified as among the key pathways and subsequently had its member proteins validated to be differentially expressed. Significant correlations between miRNA biomarkers and the TNF signaling pathway proteins' principal components might indicate their relevance in the pathogenesis of the syndrome.

Few prior studies have focused on developing leptospiral SPHS biomarkers. One study suggested platelet-activating factor acetylhydrolase, but the marker was evaluated in patients with unclear clinical manifestation of SPHS.[12] Cytokines like IL-5, IL-6, IL-8, and

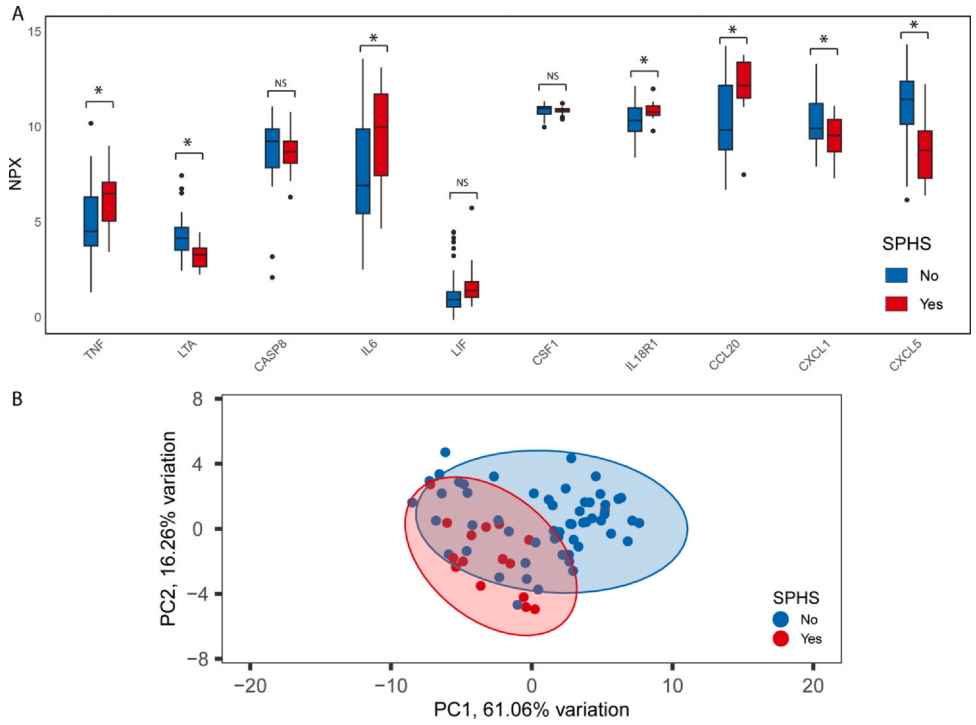

Fig. 6. Expression profile of TNF signaling pathway proteins. (A) Boxplots showing the expression levels of 10 proteins related to TNF signaling pathways. The dots represent potential outliners. The asterisks represent significant moderated t-tests, q-value < 0.05, NS: not significant, NPX: normalized protein expression unit. (B) Principal component analysis showing the clustering of SPHS and non-SPHS patients as subjected to the first two principal components. Each dot represents one patient. PC1: principal component 1, PC2: principal component 2.

IL-10 have been reported to be elevated in SPHS patients, though their predictive roles have not been assessed.[13,45] A recent study highlighted serum macrophage migration inhibitory factor for discriminating leptospirosis SPHS from other febrile illnesses, but most confirmed cases had prolonged disease duration before blood collection, limiting its predictive value.[14] Compared to current literature, the novel miRNA biomarkers were developed from a sufficient sample size with relatively large number of well-characterized SPHS cases. Their stable discriminatory performance was proven through adjustment for potential confounding effects of age, sex and recruitment sites. More importantly, the miRNAs displayed earlier change compared to routine chest X-ray imaging and had the potential to combine with other miRNAs or proteins to improve predictability and specificity.

Our study also revealed TNF signaling pathway as among the key host response mechanisms in leptospirosis SPHS, which appeared to align with existing evidence. Previous studies have confirmed the higher levels of TNF-α in leptospirosis patients than in healthy controls, with the cytokine elevation linked to bleeding and organ involvement, especially the lungs.[46,47] These finding was later reinforced by one study that observed the association between TNF-α and pulmonary hemorrhage in Weil syndrome patients.[48] Interestingly, IL6, another pathway member cytokine, was also demonstrated to be significantly upregulated in leptospiral SPHS patients in two separate studies.[13,45] These findings, along with our results, strongly underscore the importance of TNF signaling pathway in leptospirosis SPHS.

Existing evidence suggests several mechanisms on how TNF signaling pathway might contribute to alveolar-lung capillary barrier breakdown and lung hemorrhage. TNF-α is a proinflammatory cytokine that mediates the host response to facilitate pathogen clearance. However, its overexpression can lead to a cytokine storm and increased severity of illness.[49] TNF-α can stimulate the endothelium, increasing the expression of adhesion molecules and chemokines, and amplifying the inflammatory response by inducing NF-κB and MAPK signaling, which subsequently triggers the expression of additional pro-inflammatory cytokines and recruits immune cells to the site of inflammation, resulting in tissue damage and vascular leakage.[50,51] Moreover, TNF- α can alter the expression and localization of tight junction proteins between endothelial cells, increasing permeability of the endothelial barrier.[52] TNF-α can further induce the production and activation of certain members of the matrix metalloproteinase family, enzymes that degrade extracellular matrix components and play a crucial role in both injury and repair of the alveolar capillary membrane in acute lung injury.[53–55] In addition, TNF-α has been proposed to regulate the expression of the epithelial sodium channel transporter in alveolar epithelial cells and tubular cells, a mechanism implicated in pulmonary edema and acute kidney injury in leptospirosis.[56]

Our findings regarding the association between miR-147b-3p and TNF signaling pathway protein resonates well with previous studies. Liu et al. demonstrated that miR-147b production is induced by Toll-like receptor (TLR) stimulation in murine macrophages, acting as a negative feedback loop to inhibit the inflammation induced by TLR itself. Transfection of miR-147b or its mimics significantly reduced the expression of inflammatory cytokines, including TNF-α.[57] Another study confirmed miR-147b's role as an inflammatory regulator, showing it alleviates inflammation in a rat acute lung injury model and A549 cells, with TNF-α levels reduced in cells transfected with miR-147b mimics.[58] Based on this evidence, the up-regulation of miR-147b-3p seen in our study might reflect the host response to control the inflammation inflicted by the increased TNF level.

Although our most important miRNA biomarker, miR-5010–3p, has not been previously studied for its role in the inflammatory response or lung hemorrhage, its correlations with many proteins from TNF signaling pathway might suggest some potential mechanisms of action. CXCL5, a chemokine known to be induced in acute respiratory infections and produced primarily by alveolar type II epithelial cells, is a potent neutrophil attractant that affects lung inflammation trajectory.[59] It has been found to be upregulated in

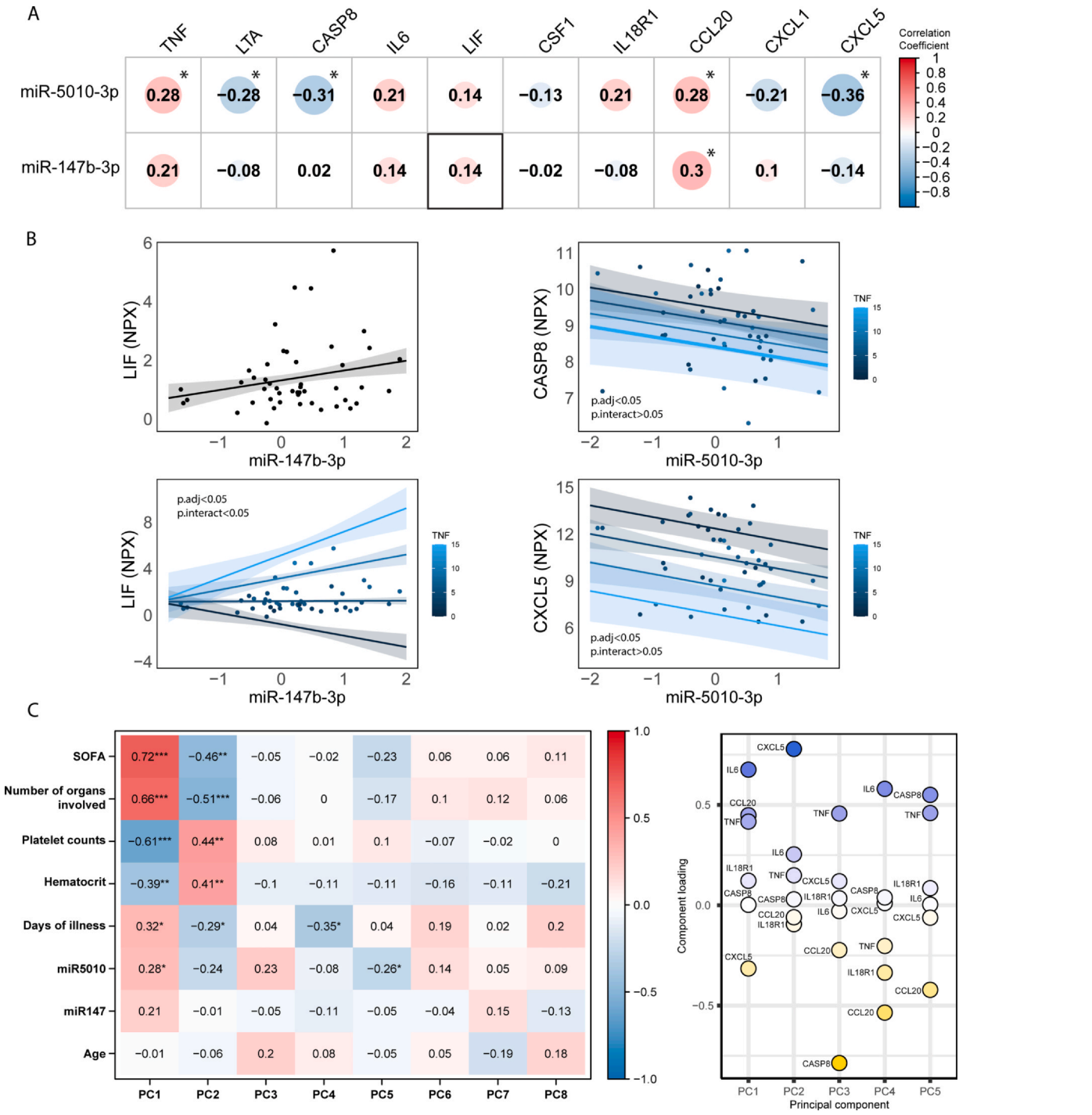

Fig. 7. MiRNA biomarkers and TNF signaling pathway proteins correlation analysis. (A) Correlation matrix between miRNAs and the 10 proteins in TNF signaling pathway. The color gradient indicates correlation coefficients, with positive value in red and negative in blue (Pearson's test). Dot size correlates with the coefficient values, which are provided as black numbers within the dot. The asterisk indicates a significant test (p-value < 0.05). The thickened outline indicates the target of the miRNAs as reference from microRNA validated target databases. (B) Scatter plot with simple linear regression LIF ~ miR-147b-3p (upper left), multivariable linear regression with a significant interaction term LIF ~ miR-147b-3p*TNF (lower left) and multivariable linear regression without a significant interaction term CASP8 ~ miR-5010–3p + TNF (upper right), CXCL5 ~ miR-5010–3p + TNF (lower right). P.adj: p-value of the corresponding miRNA covariate in the multivariable linear regression model with TNF levels. P.interact: p-value of the likelihood ratio test, which tests whether the model with an interaction term fits the data better than the model without an interaction term. NPX: normalized protein expression unit. (C) Eigencor plot (left side plot) showing the correlation between some continuous variables with the principal components of the TNF signaling pathway expression profile. The number in each tile represents the correlation coefficient of the respective continuous variable-principal component pair. The asterisks indicate significant tests (p-value < 0.05 = *, < 0.01 = **, < 0.001 = ***). Component loading plot (right side plot) showing the underlying calculations of each PC, which elaborates the contribution of the proteins to the PCs. PC: principal component. SOFA: Sequential Organ Failure Assessment.

lungs of mice resistant to Leptospira infection, but not susceptible ones, suggesting its importance to controlling Leptospira infection and lung inflammation.[60] The negative correlation between CXCL5 and miR-5010–3p might indicate an inflammation-modulating role of miR-5010–3p in patients with leptospirosis SPHS. Furthermore, significant negative correlation between miR-5010–3p and CASP8 might reveal its role in regulating cell apoptosis. The miRNA-induced suppression of cell apoptosis might either be a beneficial host

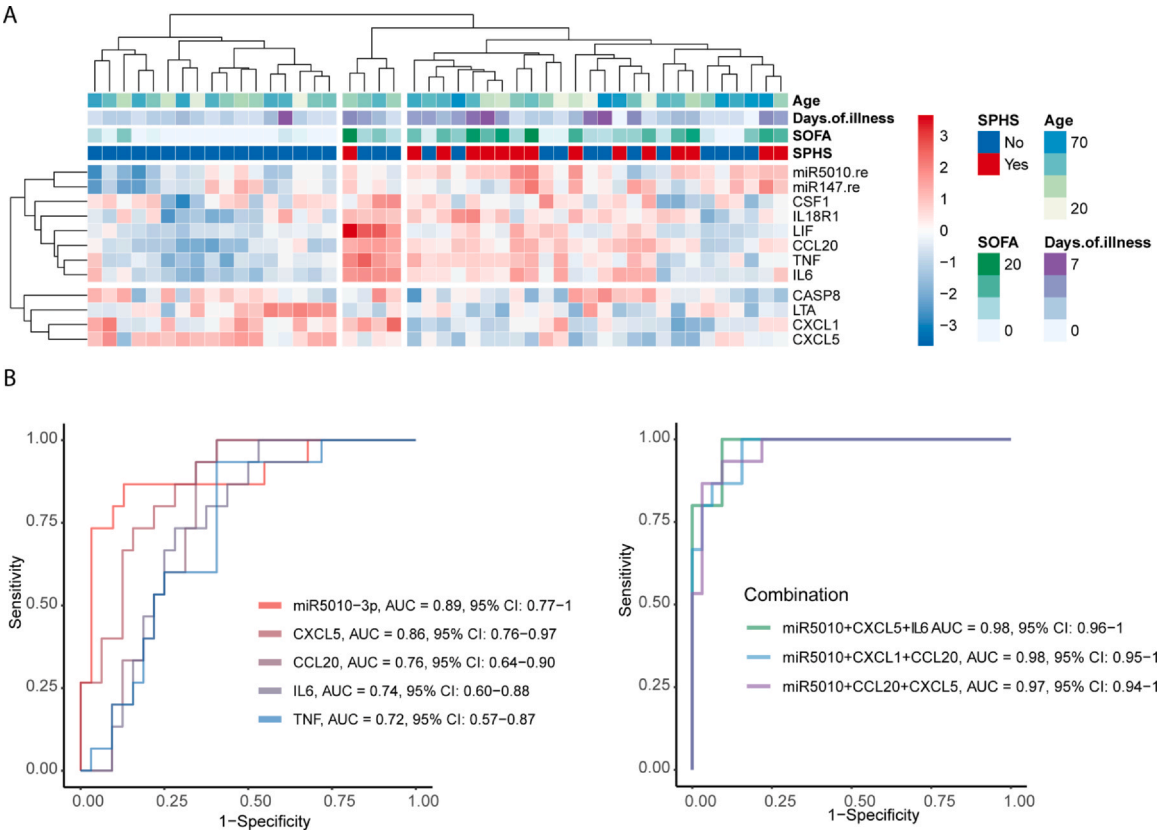

Fig. 8. Characterization of leptospirosis SPHS by miRNA biomarkers and TNF signaling pathway proteins. (A) Heatmap showing the distance clustering of miRNA biomarkers and TNF signaling pathway proteins and how they characterize SPHS phenotypes and other clinical features of leptospirosis patients. The columns were clustered using the Euclidean method incorporated in pheatmap R package. The color gradient describes the row-normalized z-score. SPHS: severe pulmonary hemorrhagic syndrome. SOFA: Sequential Organ Failure Assessment. (B) Receiver Operating Characteristics (ROC) curve analyses for single (left) and combined molecules (right). Area under the curve (AUC) values and 95% confident intervals were calculated using pROC R package.

response to counteract apoptosis signals inflicted by pathogenic Leptospira,[61,62] or it might also lead to detrimental prolonged inflammation, causing tissue damage and lung hemorrhage. Many possibilities might explain the positive correlation between miR-5010–3p and TNF, however, negative feedback might also be possible, similar to miR-147b-3p. Since the current evidence is mostly suggestive, further investigation of miR-5010–3p regulatory role via the TNF signaling pathway in leptospirosis SPHS should yield great insights into miRNA-based therapy and precision medicine in severe leptospirosis.

This study demonstrates numerous strengths. To our knowledge, it is the first investigation to specifically explore and validate the roles of circulating miRNAs as biomarkers for SPHS in patients with leptospirosis. By recruiting cases from multiple sites across Thailand, the findings are generalizable to similar healthcare settings. The sample size was carefully determined to ensure precise estimates of the AUC value and its confidence intervals. Additionally, the systems biology approach, followed by pathway protein validation, confirmed the significance of TNF signaling in SPHS and identified the potential target pathway through which the miRNA biomarkers might be involved in the pathogenesis of leptospiral SPHS.

This study has certain limitations that warrant consideration. Firstly, although the miRNAs could identify SPHS earlier than chest radiograph manifestations, most patients were admitted only after severe symptoms had already appeared. The predictive value of the miRNA biomarkers should be further confirmed in studies recruiting patients earlier in the disease course. Secondly, half of our samples showed signs of hemolysis. Although we have accounted for this using an appropriate endogenous normalizer and sensitivity analysis, contamination from red blood cell miRNAs on the circulating miRNA is possible and should be minimized in future studies. Thirdly, serum collection involves a coagulation process during which blood cells miRNAs can be released and alter circulating miRNA levels. Finally, fasting status and nutrition intake have been shown to affect circulating miRNA expression but could not be accounted for in this study.

Conclusions

MiR-5010–3p and miR-147b-3p are novel biomarkers with good predictability and potential relevance with TNF signaling pathway, an important host response mechanism in leptospirosis SPHS.

Author contributions

PNTT designed the project, defended the proposal, obtained approval from ethics review board, analyzed the data, obtained University and Faculty grants, and wrote the first draft of the manuscript. UL conducted the miRNAs experiments and oversaw the data analysis. JD and ST conducted the miRNAs extraction and managed the biorepository and clinical data of the included patients. TS and CD oversaw the data collection. SR conducted the proteomics experiments. NS directed the study. DH, UL, and NS contributed to the writing and revision of the manuscript. PNTT, UL, and JD accessed and verified the data. All authors had full access to all the data in the study and had final responsibility for the decision to submit for publication.

Funding

This research was supported by NIH/NIAID R01 AI183353 (U.L., N.S., and D.A.H.) and NIH/NIAID P01 AI168148 (U.L., N.S., and D.A.H.). This study was also supported by the 90th Anniversary of Chulalongkorn University Fund (Ratchadaphiseksomphot Endowment Fund), the Ratchadapiseksompotch Fund, Graduate Affairs, Faculty of Medicine, Chulalongkorn University (Grant number GA67/040), and the Second Century Fund (C2F), Chulalongkorn University (U.L.).

Data availability

The Nanostring microRNA profiling data was deposited at the NCBI Gene Expression Omnibus (GEO), accession ID GSE283845. The LC-MS/MS data have been deposited to the ProteomeXchange Consortium via the PRIDE partner repository with the dataset identifier PXD052319. All other data was available on reasonable request to the corresponding author.

Declaration of Competing Interest

The authors declare that they have no known competing financial interests or personal relationships that could have appeared to influence the work reported in this paper.

Acknowledgments

We express our gratitude to Chulalongkorn University for awarding the research scholarships and NIH grant support. We would also like to extend our appreciation to the clinicians and nurses, particularly Dr. Sakarin Boonprasong from Sisaket Provincial Public Health Office, Sisaket, Thailand; Ms. Piyada Sornpood, M.N.S, from Srisaket province, Thailand; and Ms. Jaru Suwanpakdee from Thungsong Hospital, Nakhon Si Thammarat, Thailand, for their assistance in data collection and patient follow-up processes. Our sincere thanks go to all the patients and their next of kin for their participation in this research. Furthermore, we are grateful to the National Center for Genetic Engineering and Biotechnology (BIOTEC) for their invaluable consultation regarding proteomics experiments and for conducting the MALDI-TOF and LC-MS/MS proteomics. Special thanks are extended to Prof. Janet C. Lindow for providing the clinical data of the patients in the transcriptomics experiment.

Appendix A. Supporting information

Supplementary data associated with this article can be found in the online version at doi:10.1016/j.jinf.2024.106400.

References

1. Torgerson PR, Hagan JE, Costa F, Calcagno J, Kane M, Martinez-Silveira MS, et al. *Global burden of leptospirosis: estimated in terms of disability adjusted life years. PLoS Negl Trop Dis* 2015;**9**(10):0004122.
2. Costa F, Hagan JE, Calcagno J, Kane M, Torgerson P, Martinez-Silveira MS, et al. *Global morbidity and mortality of leptospirosis: a systematic review. PLoS Negl Trop Dis* 2015;**9**(9):0003898.
3. Panaphut T, Domrongkitchaiporn S, Thinkamrop B. *Prognostic factors of death in leptospirosis: a prospective cohort study in Khon Kaen, Thailand. Int J Infect Dis* 2002;**6**(1):52–9.
4. Gouveia EL, Metcalfe J, De Carvalho AL, Aires TS, Villasboas-Bisneto JC, Queirroz A, et al. *Leptospirosis-associated severe pulmonary hemorrhagic syndrome, Salvador, Brazil. Emerg Infect Dis* 2008;**14**(3):505–8.
5. Haake DA, Levett PN. *Leptospirosis in Humans.* In: Adler B, editor. Leptospira and Leptospirosis. Berlin, Heidelberg: Springer Berlin Heidelberg; 2015. p. 65–97.
6. Marchiori E, Lourenço S, Setúbal S, Zanetti G, Gasparetto TD, Hochhegger B. *Clinical and imaging manifestations of hemorrhagic pulmonary leptospirosis: a state-of-the-art review. Lung* 2011;**189**(1):1–9.
7. Du Couedic L, Courtin J, Poubeau P, Tanguy B, Di Francia M, Arvin-Berod C. *Patent and occult intra-alveolar hemorrhage in leptospirosis. Rev Mal Respir* 1998;**15**(1):61–7.
8. Paganin F, Bourdin A, Dalban C, Courtin JP, Poubeau P, Borgherini G, et al. *Leptospirosis in Reunion Island (Indian Ocean): analysis of factors associated with severity in 147 confirmed cases. Intensive Care Med* 2007;**33**(11):1959–66.
9. Marotto PC, Ko AI, Murta-Nascimento C, Seguro AC, Prado RR, Barbosa MC, et al. *Early identification of leptospirosis-associated pulmonary hemorrhage syndrome by use of a validated prediction model. J Infect* 2010;**60**(3):218–23.
10. So RAY, Danguilan RA, Chua E, Arakama M-HI, Ginete-Garcia JKB, Chavez JR. *A scoring tool to predict pulmonary complications in severe leptospirosis with kidney failure. Trop Med Infect Dis* 2022;**7**(1):7.
11. Sonderegger F, Nentwig A, Schweighauser A, Francey T, Marti E, Mirkovitch J, et al. *Association of markers of endothelial activation and dysfunction with occurrence and outcome of pulmonary hemorrhage in dogs with leptospirosis. J Vet Intern Med* 2021;**35**(4):1789–99.
12. Yang J, Zhang Y, Xu J, Geng Y, Chen X, Yang H, et al. *Serum activity of platelet-activating factor acetylhydrolase is a potential clinical marker for leptospirosis pulmonary hemorrhage. PLoS One* 2009;**4**(1):4181.
13. Reis EA, Hagan JE, Ribeiro GS, Teixeira-Carvalho A, Martins-Filho OA, Montgomery RR, et al. *Cytokine response signatures in disease progression and development of severe clinical outcomes for leptospirosis. PLoS Negl Trop Dis* 2013;**7**(9):2457.
14. Sumaiya K, Akino Mercy CS, Muralitharan G, Hajinur Hirad A, Alarfaj AA, Natarajaseenivasan K. *Assessment of serum macrophage migration inhibitory factor (MIF) as an early diagnostic marker of leptospirosis. Front Cell Infect Microbiol* 2021;**11**:781476. 781476.
15. Wu Y, Li Q, Zhang R, Dai X, Chen W, Xing D. *Circulating microRNAs: biomarkers of disease. Clin Chim Acta* 2021;**516**:46–54.
16. Grasedieck S, Sorrentino A, Langer C, Buske C, Döhner H, Mertens D, et al. *Circulating microRNAs in hematological diseases: principles, challenges, and perspectives. Blood* 2013;**121**(25):4977–84.
17. Limothai U, Jantarangsi N, Suphavejkornkij N, Tachaboon S, Dinhuzen J, Chaisuriyong W, et al. *Discovery and validation of circulating miRNAs for the clinical prognosis of severe dengue. PLoS Negl Trop Dis* 2022;**16**(10):0010836.
18. Limothai U, Dinhuzen J, Payongsri T, Tachaboon S, Tangkijvanich P, Chuaypen N, et al. *Circulating microtranscriptome profiles reveal distinct expression of microRNAs in severe leptospirosis. PLoS Negl Trop Dis* 2020;**14**(11):0008809.
19. Phannajit J, Lertussavavivat T, Limothai U, Tachaboon S, Avihingsanon Y, Praditpornsilpa K, et al. *Long-term kidney outcomes after leptospirosis: a prospective multicentre cohort study in Thailand. Nephrol Dial Transplant* 2023;**38**(10):2182–91.
20. Herath N, Uluwattage W, Weliwitiya T, Karunanayake L, Lekamwasam S, Ratnatunga N, et al. *Sequel and therapeutic modalities of leptospirosis associated severe pulmonary haemorrhagic syndrome (SPHS); a Sri Lankan experience. BMC Infect Dis* 2019;**19**(1):451.
21. Fonseka CL, Dahanayake NJ, Mihiran DJD, Wijesinghe KM, Liyanage LN, Wickramasuriya HS, et al. *Pulmonary haemorrhage as a frequent cause of death among patients with severe complicated Leptospirosis in Southern Sri Lanka. PLoS Negl Trop Dis* 2023;**17**(10):0011352.
22. Mei Q, Li X, Meng Y, Wu Z, Guo M, Zhao Y, et al. *A facile and specific assay for quantifying microRNA by an optimized RT-qPCR approach. PLoS One* 2012;**7**:e46890.
23. MacLellan SA, MacAulay C, Lam S, Garnis C. *Pre-profiling factors influencing serum microRNA levels. BMC Clin Pathol* 2014;**14**:1–11.
24. Shah JS, Soon PS, Marsh DJ. *Comparison of methodologies to detect low levels of hemolysis in serum for accurate assessment of serum microRNAs. PLoS One* 2016;**11**(4):0153200.
25. Parker VL, Gavriil E, Marshall B, Pacey A, Heath PR. *Profiling microRNAs in uncomplicated pregnancies: serum vs. plasma. Biomed Rep* 2021;**14**(2):24.
26. Petersen PH, Lopacinska-Jørgensen J, Høgdall CK, Høgdall EV. *Identification of stably expressed microRNAs in plasma from high-grade serous ovarian carcinoma and benign tumor patients. Mol Biol Rep* 2023;**50**(12):10235–47.
27. Blondal T, Jensby Nielsen S, Baker A, Andreasen D, Mouritzen P, Wrang Teilum M, et al. *Assessing sample and miRNA profile quality in serum and plasma or other biofluids. Methods* 2013;**59**(1):S1–6.
28. Chen X, Ba Y, Ma L, Cai X, Yin Y, Wang K, et al. *Characterization of microRNAs in serum: a novel class of biomarkers for diagnosis of cancer and other diseases. Cell Res* 2008;**18**(10):997–1006.
29. Kirschner MB, Kao SC, Edelman JJ, Armstrong NJ, Vallely MP, van Zandwijk N, et al. *Haemolysis during sample preparation alters microRNA content of plasma. PLoS One* 2011;**6**(9):24145.
30. Lindow JC, Wunder EA Jr. Jr, Popper SJ, Min JN, Mannam P, Srivastava A, et al. *Cathelicidin insufficiency in patients with fatal leptospirosis. PLoS Pathog* 2016;**12**(11):1005943.
31. Jin L, Bi Y, Hu C, Qu J, Shen S, Wang X, et al. *A comparative study of evaluating missing value imputation methods in label-free proteomics. Sci Rep* 2021;**11**(1):1760.
32. Ritchie ME, Phipson B, Wu D, Hu Y, Law CW, Shi W, et al. *limma powers differential expression analyses for RNA-sequencing and microarray studies. Nucleic Acids Res* 2015;**43**(7):47. e47-e.
33. Dabney A, Storey JD, Warnes G. *Q-value estimation for false discovery rate control. Medicine* 2004;**344**(539):48.
34. Kevin Blighe AL. PCAtools: everything Principal Component Analysis; 2023. https://doi.org/10.18129/B9.bioc.PCAtools. Accessed date: 01/03/2024.
35. Huang HY, Lin YC, Cui S, Huang Y, Tang Y, Xu J, et al. *miRTarBase update 2022: an informative resource for experimentally validated miRNA-target interactions. Nucleic Acids Res* 2022;**50**(D1):D222–30.
36. Skoufos G, Kakoulidis P, Tastsoglou S, Zacharopoulou E, Kotsira V, Miliotis M, et al. *TarBase-v9.0 extends experimentally supported miRNA–gene interactions to cell-types and virally encoded miRNAs. Nucleic Acids Res* 2023;**52**(D1):D304–10.

37. Kanehisa M, Furumichi M, Sato Y, Kawashima M, Ishiguro-Watanabe M. *KEGG for taxonomy-based analysis of pathways and genomes. Nucleic Acids Res* 2023;**51**(D1):D587–92.
38. Paczkowska M, Barenboim J, Sintupisut N, Fox NS, Zhu H, Abd-Rabbo D, et al. *Integrative pathway enrichment analysis of multivariate omics data. Nat Commun* 2020;**11**(1):735.
39. Kanehisa M, Sato Y, Kawashima M. *KEGG mapping tools for uncovering hidden features in biological data. Protein Sci* 2022;**31**(1):47–53.
40. Robin X, Turck N, Hainard A, Tiberti N, Lisacek F, Sanchez JC, et al. *pROC: an open-source package for R and S+ to analyze and compare ROC curves. BMC Bioinformatics* 2011;**12**(1):77.
41. Takizawa S, Matsuzaki J, Ochiya T. *Circulating microRNAs: challenges with their use as liquid biopsy biomarkers. Cancer Biomark* 2022;**35**(1):1–9.
42. Romaine SPR, Charchar FJ, Samani NJ, Tomaszewski M. *Circulating microRNAs and hypertension—from new insights into blood pressure regulation to biomarkers of cardiovascular risk. Curr Opin Pharmacol* 2016;**27**:1–7.
43. Picchio V, Ferrero G, Cozzolino C, Pardini B, Floris E, Tarallo S, et al. *Effect of traditional or heat-not-burn cigarette smoking on circulating miRNAs in healthy subjects. Eur J Clin Investig* 2024;**54**(4):14140. e14140.
44. Raftery AE, Painter IS, Volinsky CT. BMA: an R package for Bayesian model averaging. *The Newsletter of the R Project Volume*; 2005; 5(2). https://CRAN.R-project.org/package=BMA. Accessed date: 01/03/2024.
45. Limothai U, Lumlertgul N, Sirivongrangson P, Kulvichit W, Tachaboon S, Dinhuzen J, et al. *The role of leptospiremia and specific immune response in severe leptospirosis. Sci Rep* 2021;**11**(1):14630.
46. Estavoyer J, Racadot E, Couetdic G, Leroy J, Grosperrin L. *Tumor necrosis factor in patients with leptospirosis. Rev Infect Dis* 1991;**13**(6):1245–6.
47. Tajiki H, Salomão R. *Association of plasma levels of tumor necrosis factor alpha with severity of disease and mortality among patients with leptospirosis. Clin Infect Dis* 1996;**23**:1177–8.
48. Kyriakidis I, Samara P, Papa A. *Serum TNF-α, sTNFR1, IL-6, IL-8 and IL-10 levels in Weil's syndrome. Cytokine* 2011;**54**(2):117–20.
49. Cagliero J, Villanueva SY, Matsui M. *Leptospirosis pathophysiology: into the storm of cytokines. Front Cell Infect Microbiol* 2018;**8**:204.
50. Pober JS. *Endothelial activation: intracellular signaling pathways. Arthritis Res* 2002;**4 3**(3):109–16.
51. Webster JD, Vucic D. *The balance of TNF mediated pathways regulates inflammatory cell death signaling in healthy and diseased tissues. Front Cell Dev Biol* 2020;**8**:365.
52. Mazzon E, Cuzzocrea S. *Role of TNF-alpha in lung tight junction alteration in mouse model of acute lung inflammation. Respir Res* 2007;**8**(1):75.
53. Han Y-P, Tuan T-L, Wu H, Hughes M, Garner WL. *TNF-α stimulates activation of pro-MMP2 in human skin through NF-κB mediated induction of MT1-MMP. J Cell Sci* 2001;**114**(1):131–9.
54. Lee IT, Lin CC, Wu YC, Yang CM. *TNF-alpha induces matrix metalloproteinase-9 expression in A549 cells: role of TNFR1/TRAF2/PKCalpha-dependent signaling pathways. J Cell Physiol* 2010;**224**(2):454–64.
55. Davey A, McAuley DF, O'Kane CM. *Matrix metalloproteinases in acute lung injury: mediators of injury and drivers of repair. Eur Respir J* 2011;**38**(4):959–70.
56. Dagenais A, Fréchette R, Yamagata Y, Yamagata T, Carmel JF, Clermont ME, et al. *Downregulation of ENaC activity and expression by TNF-α in alveolar epithelial cells. Am J Physiol Lung Cell Mol Physiol* 2004;**286**(2):L301–11.
57. Liu G, Friggeri A, Yang Y, Park Y-J, Tsuruta Y, Abraham E. *miR-147, a microRNA that is induced upon Toll-like receptor stimulation, regulates murine macrophage inflammatory responses. Proc Natl Acad Sci* 2009;**106**(37):15819–24.
58. Xu Q, Huang G-D, Duan G-C, Qin H-J. *MicroRNA-147b alleviates inflammation and apoptosis in acute lung injury via inhibition of p38 MAPK signaling pathway. Eur Rev Med Pharmacol Sci* 2021;**25**(4):1974–81.
59. Jeyaseelan S, Manzer R, Young SK, Yamamoto M, Akira S, Mason RJ, et al. *Induction of CXCL5 during inflammation in the rodent lung involves activation of alveolar epithelium. Am J Respir Cell Mol Biol* 2005;**32**(6):531–9.
60. Domingos RH, Pavanel EB, Nakajima E, Schons-Fonseca L, Da Costa R, De Franco M, et al. *Resistance of mice to Leptospira infection and correlation with chemokine response. Immunobiology* 2017;**222**(11):1004–13.
61. Che R, Ding S, Zhang Q, Yang W, Yan J, Lin Xa. *Haemolysin Sph2 of Leptospira interrogans induces cell apoptosis via intracellular reactive oxygen species elevation and mitochondrial membrane injury. Cell Microbiol* 2019;**21**(1):12959.
62. Jin D, Ojcius DM, Sun D, Dong H, Luo Y, Mao Y, et al. *Leptospira interrogans induces apoptosis in macrophages via caspase-8-and caspase-3-dependent pathways. Infect Immun* 2009;**77**(2):799–809.